Chemical Science

ROYAL SOCIETY OF CHEMISTRY

EDGE ARTICLE

View Article Online
View Journal | View Issue

Cite this: *Chem. Sci.*, 2024, **15**, 8500

All publication charges for this article have been paid for by the Royal Society of Chemistry

$KBa_3M_2F_{14}Cl$ (M = Zr, Hf): novel short-wavelength mixed metal halides with the largest second-harmonic generation responses contributed by mixed functional moieties†

Mei Yan,‡[a] Chun-Li Hu,‡[b] Ru-Ling Tang, *[a] Wen-Dong Yao,[a] Wenlong Liu [a] and Sheng-Ping Guo *[a]

Received 22nd February 2024
Accepted 29th April 2024

DOI: 10.1039/d4sc01259c

rsc.li/chemical-science

The development of short-wavelength nonlinear optical (NLO) materials is indispensable and urgently required for further applications. Halides have been disregarded as potential NLO materials with deep-ultraviolet (DUV) cutoff edges due to their weak second-harmonic generation (SHG) response and poor birefringence. Here, two novel and isostructural halides, $KBa_3M_2F_{14}Cl$ (M = Zr (KBZFC), Hf (KBHFC)), possess structures that are formed by isolated MF_7 monocapped triangular prisms and dissociative K^+, Ba^{2+}, and Cl^- ions. Compared with reported metal halides that are transparent to the DUV region, KBZFC and KBHFC possess the strongest SHG responses (approximately 1, 0.9 × KH_2PO_4), which are contributed by the synergistic effect of MF_7 (M = Zr, Hf) groups, Ba^{2+} cations, and Cl^- ions. The zero-dimensional structures favour sufficient birefringences (0.12, 0.10 @ 1064 nm) for phase-matchable (PM) behaviours. The discovery of KBZFC and KBHFC showcases the potential of NLO mixed metal halides transparent to the DUV region.

Introduction

Nonlinear optical (NLO) materials are variable frequency crystals that play an indispensable role in modern laser science and technology.[1–7] In the past few decades, new NLO materials with balanced performances have been vigorously explored, and deep-ultraviolet (DUV) NLO transparent materials (wavelength < 200 nm) have been applied in a range of cutting-edge fields such as semiconductor manufacturing, photolithography, advanced scientific research, and laser communication.[8–15]

Nevertheless, it is particularly difficult to design functioning DUV transparent NLO materials because of the conflict between the short UV cutoff edge (λ < 200 nm) and the large second-harmonic generation (SHG) effect ($d_{ij} > d_{36}$ (KH_2PO_4 (KDP)) = 0.39 pm V^{-1}), along with the phase-matchable (PM) ability.[16–22] Currently, only $KBe_2BO_3F_2$ (KBBF) has been commercially applied and can realize DUV laser conversion *via* a direct SHG process. However, its layered habit and highly toxic raw materials hinder its further development.[23] Therefore, there is an urgent need to develop high-performance NLO materials with a DUV cutoff edge beyond that of KBBF.

At the present stage, π-conjugated systems with planar building units, that is, borates, carbonates, nitrates, and their derivates, are promising candidates for NLO materials because of their strong SHG intensities and large birefringences.[24–29] Non-π-conjugated systems are also considered as potential systems in the DUV region because the relatively low electron energy of the σ bonds of the tetrahedral groups is conducive to a large band gap, *viz.*, a short UV cutoff edge.[30–33] Related studies and many materials with excellent NLO properties have been reported, including $K_2Al_2B_2O_7$,[34] β-$Rb_2Al_2B_2O_7$,[34] Li_2BaSiO_4,[35] $MgB_5O_7F_3$,[36] CsB_4O_6F,[12] and $K_3Sc_3(PO_4)(PO_3F)_2F_5$.[9] The materials with fluorinated oxygen-containing building units catch our attention because elemental F possesses the largest electronegativity and the highest occupied molecular orbital-lowest unoccupied molecular orbital (HOMO–LUMO) gap that is beneficial for the blueshift of UV cutoff edges,[37–40] which suggests whether metal halides can be applied in the DUV region.

To date, few metal fluorides have been reported with DUV cutoff edges, namely, $BaMgF_4$, $SrAlF_5$, $BaZnF_4$, Li_2CaMF_8 (M = zirconium (Zr), hafnium (Hf)), and $K_3Ba_2Zr_6F_{31}$.[41–45] However, $BaMgF_4$, $SrAlF_5$, and $BaZnF_4$ show weak SHG intensities (0.085, 0.65, 0.16 × KDP) and poor birefringences (0.0077, 0.0242, 0.0164) that are insufficient for PM behavior. Li_2CaMF_8 (M = Zr,

[a]*School of Chemistry and Chemical Engineering, Yangzhou University, 180 Siwangting Road, Yangzhou 225002, China. E-mail: rltang@yzu.edu.cn; spguo@yzu.edu.cn*

[b]*State Key Laboratory of Structural Chemistry, Fujian Institute of Research on the Structure of Matter, Chinese Academy of Sciences, Fuzhou, Fujian 350002, China*

† Electronic supplementary information (ESI) available: Experimental section, and additional tables and figures. CCDC 2283473 and 2311168. For ESI and crystallographic data in CIF or other electronic format see DOI: https://doi.org/10.1039/d4sc01259c

‡ These authors contributed equally.

Hf) and $K_3Ba_2Zr_6F_{31}$ were newly reported by our group, and were synthesized by introducing transition metals (TMs) Zr and Hf into halides for remarkable benefits, as follows. (1) Asymmetric d^0-TMs-based building units are conducive to the formation of noncentrosymmetric (NCS) structures.[46–48] (2) The interaction of elemental Zr and Hf with weak electronegativity and F atoms tends to blueshift the cutoff edge of the materials. (3) Zr and Hf halides tend to possess various polyhedral units and bonding modes, which can form zero-, one-, two-, and three-dimensional frameworks.

Most of the Zr and Hf halides form low-dimensional structures,[49] and the large anisotropy is in favor of perfecting the shortcomings of the non-PM behavior of reported fluorides with a DUV cutoff edge.[50] Nevertheless, Li_2CaMF_8 (M = Zr, Hf) and $K_3Ba_2Zr_6F_{31}$ show moderate SHG intensity (0.36, 0.30, and 0.5 × KDP) at 1064 nm. To further boost the SHG efficiency of halides, the Cl atom is incorporated because of its favorable chemical covalence and flexibility, and relatively large polarizability,[51] which has been proven by mixed metal halides showing improved overall NLO performance involving $Pb_{18}O_8Cl_{15}I_5$,[52] $Rb_2CdBr_2I_2$,[53] $Cs_2HgI_2Cl_2$,[54] $Pb_7F_{12}Cl_2$,[55] and $CsZnBO_3X_2$ (X_2 = F_2, Cl_2, and FCl).[56]

Guided by these considerations, our group postulated that the combination of Zr and Hf atoms with alkali/alkaline earth metal cations with full shells, as well as mixed halogen anions, is beneficial for obtaining new NLO materials with a large SHG intensity and short UV cutoff edge. Accordingly, our extensive explorations resulted in the discovery of two novel and isostructural halides, $KBa_3M_2F_{14}Cl$ (M = Zr (KBZFC), Hf (KBHFC)). Remarkably, as the first mixed metal halides reached the DUV region, KBZFC and KBHFC exhibited strong SHG effects (1.0, 0.9 × KDP) and large birefringences (0.12, 0.10 @ 1064 nm). The syntheses, crystal structures, theoretical calculations, and the structure–property relationships of KBZFC and KBHFC are described in detail in this work.

Results and discussion

Single crystals of KBZFC and KBHFC were obtained by hydrothermal synthesis (for additional details, see the ESI†). The purities of the samples were confirmed by powder X-ray diffraction (PXRD) (Fig. S1a and b†). Elemental analyses revealed the presence of K, Ba, Zr/Hf, F, and Cl elements in single crystals of KBZFC and KBHFC (Fig. S1c and d†), which conformed to the results of single crystal X-ray diffraction (SCXRD) analyses.

Crystallographic analyses (Table S1†) reveal that KBZFC and KBHFC belong to the tetragonal system with NCS space group $P\bar{4}m2$ (No. 81). Since they are isostructural, KBZFC was chosen and is described in detail. The asymmetric unit consists of two Ba, one Zr, one K, one Cl, and three F atoms, and the isotropic atomic displacement parameters (ADP) for atoms are all regular (Table S2 and Fig. S2†). As illustrated in Fig. 1, the Zr^{4+} ion is coordinated with seven fluorine atoms to form a ZrF_7 monocapped triangular prism with three sets of Zr–F bond lengths (2.130(3), 2.056(2), and 2.025(3) Å) (Table S3†). These ZrF_7 monocapped triangular prisms are isolated and arranged along the *c* axis with a slight difference in direction, as evident from the orientation of the F(1) (cap) and its opposite side formed by F(3) atoms (Fig. S3†).

The K^+, Ba^{2+}, and Cl^- ions reside in the interval of the zero-dimensional (0D) framework, compensating for the charge. Each K atom is twelve-coordinated with fluorine atoms to form a KF_{12} icosahedron, with K–F bond lengths of 2.8997(4) and 2.9184(17) Å. The Ba(1) atom is twelve-coordinated with ten F and two Cl atoms, with Ba–F bond distances in the range of 2.721(3)–3.3091(14) Å and Ba–Cl bonds of 3.18278(18) Å. Each Ba(2) atom is bonded to twelve F atoms, with bond lengths ranging from 2.8997(4) to 2.7739(17) Å. It should be noted that the Cl atom only bonds to the Ba(1) atom, which can be seen as dissociative in the interspace. The bond valence sum (BVS) results for K^+, Ba^{2+}, Zr^{4+}/Hf^{4+}, F^-, and Cl^- ions are 0.97, 2.13–2.23, 4.00, 0.93–1.09, and 1.06 for KBZFC, and 0.98, 2.11–2.25, 4.12, 0.82–0.97, 1.08 for KBHFC, respectively (Table S2†).[57]

Related information for NCS halides with mixed fluorine and chlorine atoms are summarized in Table S4,† and six of them belong to the tetrahedral system (*I*4: $SbCl_3F_2$,[58] $SbF_{1.6}Cl_{3.4}$,[59] $I\bar{4}$:$TaCl_4F$,[60] $SbCl_4F$,[61] $SbCl_3F_2$,[62] and $I\bar{4}2m$: $CsSbF_3Cl$[63]). They show similar 0D structures, and a representative of the group, $CsSbF_3Cl$, is composed of four fundamental building units, the $[SbF_3Cl_2]$ anionic group, which is interconnected by shared F atoms that form isolated $[Sb_4F_{12}Cl_4]$ units. Apparently, the Cl atoms are coordinated atoms, and are distinguished from the dissociative atoms in KBZFC and KBHFC. As summarized in

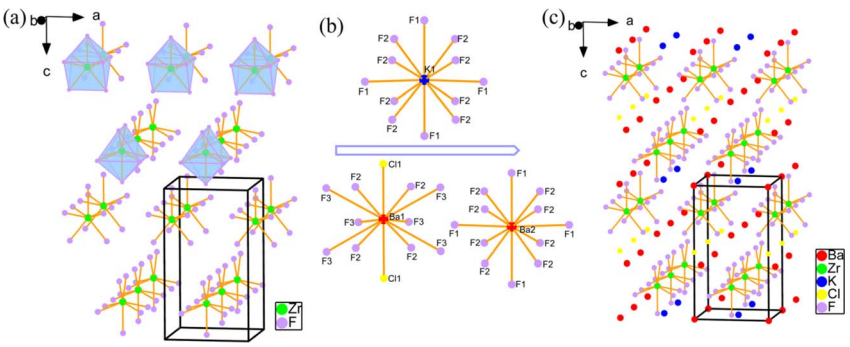

Fig. 1 (a) Isolated ZrF_7 monocapped triangular prisms. (b) Coordination modes of K^+ and Ba^{2+} cations. (c) The structure of KBZFC.

Table S5,† mixed metal halides exhibit various structures and excellent NLO properties. $Pb_7F_{12}Cl_2$ and $Pb_7F_{12}Br_2$ display large rings formed by $[Pb_7F_{24}]^{10-}$ units, and Cl/Br atoms fill in the middle of the rings.[55,64] Nevertheless, the MF_7 units in KBZFC and KBHFC form the 0D structure that compensates for large anisotropy.

Compared with $K_3Ba_2Zr_6F_{31}$,[45] the incorporation of Cl^- anion largely changes the crystal structure and dimension. Specifically, $K_3Ba_2Zr_6F_{31}$ features $\{[Zr_6F_{31}]^{7-}\}_\infty$ chains formed by *cis*-$[Zr_6F_{34}]^{10-}$ clusters, with K^+ and Ba^{2+} cations situated between the chains. KBZFC and KBHFC characterize the 0D structure composed of MF_7 units because the Cl^- anions are not connected to Zr/Hf atoms. In terms of element composition, KBZFC and KBHFC are firstly combined by alkali, alkaline earth, d^0-TMs, and mixed halogens. Additionally, they are firstly reported as NLO mixed metal halides that extend to the DUV region.

The recorded UV-vis-NIR diffuse reflectance spectra of KBZFC and KBHFC are displayed in Fig. 2a and show no obvious absorption peak in the range of 200–800 nm, which indicates a short UV cutoff edge below 200 nm and high reflectance of 73% and 72%, respectively. Additionally, crystals with sizes of 3 × 3 × 0.4 mm for KBZFC and 5 × 4 × 0.4 mm for KBHFC were used to collect their transmittance spectra in the range of 190–800 nm. The values are 194 and 192.8 nm, which confirm their DUV transparency capability (Fig. 2b). Apparently, KBZFC and KBHFC are the first mixed metal halides that extend to the DUV region (Fig. 2c). The symmetric stretching of the Zr/Hf–F bond was observed at 434/458 cm^{-1},[65] and the IR-transparent regions of KBZFC and KBHFC span from 2.5 to 23.0 μm (2.7 to 23.0 μm) (Fig. S4†).

According to the thermogravimetric curves, KBZFC and KBHFC are thermostable up to 362 °C and 353 °C, respectively. They displayed similar decomposition curves corresponding to the loss of $ZrCl_4$/$HfCl_4$ and ZrF_4/HfF_4 molecules from 362/353 °C to 1000 °C (Fig. S5a and b†). After heating to 1000 °C, the remaining product was Ba_2ZrF_8/Ba_2HfF_8 and some unknown phases (Fig. S5c and d†).

Because KBZFC and KBHFC crystallize in the NCS space group, the SHG measurements were estimated under 1064 nm laser radiation based on the Kurtz–Perry method.[66] A polycrystalline sample of KDP was utilized as a reference during the test. The results indicate that KBZFC and KBHFC feature PM behaviour and exhibit large SHG effects approximately 1.0 and 0.9 times that of KDP, respectively (Fig. 3). To date, only three of the thirty-two reported NCS metal halides with mixed fluorine and chlorine have been found to be SHG-active,[50,55,63] and their absorption is confined to the UV and even visible regions (Table S4†). Additionally, the NLO properties of other NCS halides with mixed halogens are summarized in Table S5,† which highlights KBZFC and KBHFC as the first to reach the DUV region, and they show the largest SHG effects among all the reported metal halides with DUV cutoff edges.

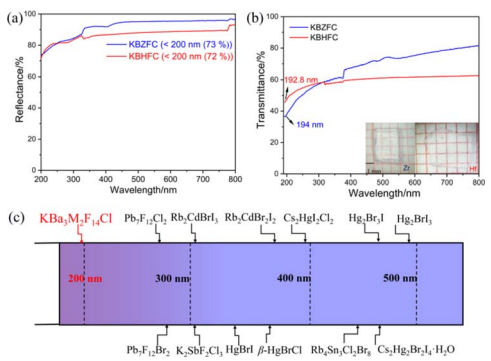

Fig. 2 (a) UV-vis-NIR diffuse reflectance spectra of KBZFC and KBHFC. (b) DUV transmittance spectra of KBZFC and KBHFC. (c) Comparison of the absorption edges of KBZFC and KBHFC with reported mixed metal halides.

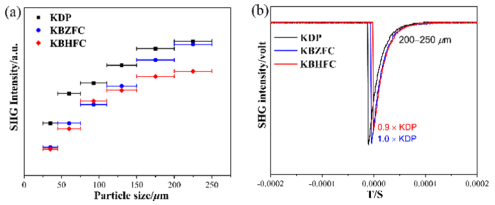

Fig. 3 (a) Powder SHG measurements of KDP, KBZFC, and KBHFC at 1064 nm. (b) SHG signals from KBZFC and KBHFC compared with benchmark KDP at 200–250 μm.

The birefringences of KBZFC and KBHFC were measured by polarized light microscope at 546 nm (Fig. S6†). The crystal thicknesses are 6.75 and 8.17 μm, and the optical path differences are 0.739 and 0.738 μm. As a result, the experimental birefringences of KBZFC and KBHFC are 0.11 and 0.09 @ 546 nm, respectively.[67]

To further elucidate the microscopic mechanism of the optical properties of KBZFC and KBHFC, density functional theory (DFT) was used to examine the electronic structures. The band structure analyses reveal that KBZFC and KBHFC are indirect band gap materials because the valence band (VB) and the conduction band (CB) are located at different *k* points (G to X), with bandgap values of 5.43 and 6.03 eV, respectively (Fig. S7a and S7b†). These values are smaller than the experimental values (6.39, 6.43 eV) and are reasonable for the limitation of the exchange and correlation function of the generalized gradient approximation–Perdew-Burke–Ernzerhof (GGA-PBE).

For interpretation of the charge transfer among the component atoms, the total density of states (DOS) and partial density of states (PDOS) of KBZFC and KBHFC are presented in Fig. S7c and d.† The upper region of the VB and the bottom of the CB were taken into consideration for the optical properties only related to the vicinity of the forbidden band. The VB from −5 eV to the Fermi level was mainly contributed by the Cl 3p nonbonding states, while the CB was mainly derived from unoccupied Zr 4d/Hf 5d and F 2p orbitals. Therefore, the band gaps of KBZFC and KBHFC were determined by the MF_7 (M = Zr, Hf) units and Cl^- anions.

Restricted by tetragonal space group $P\bar{4}m2$, KBZFC and KBHFC exhibit two nonzero tensors d_{14} and d_{36}. The maximum calculated values are 0.8665 pm V^{-1} (2.2 × KDP) for KBZFC and

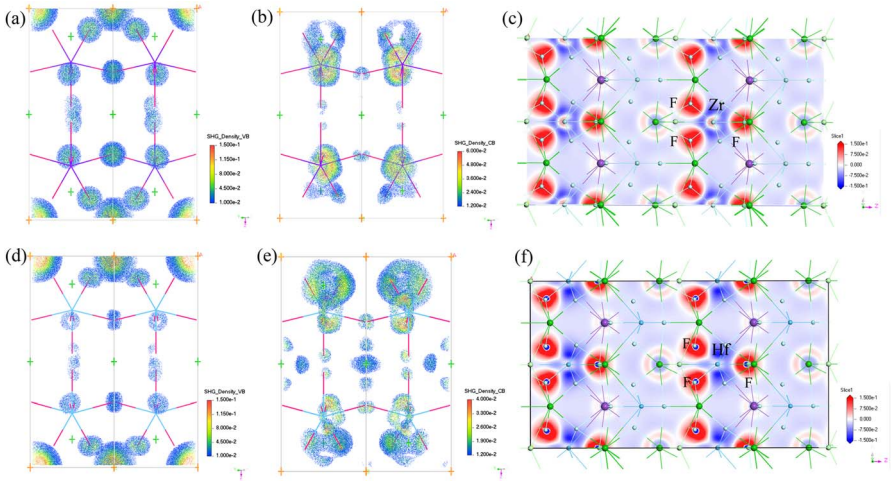

Fig. 4 SHG density in (a and d) VBs and (b and e) CBs. (c and f) EDD maps of KBZFC and KBHFC.

$d_{31} = 0.6875$ pm V^{-1} (1.75 × KDP) for KBHFC, which are larger than the experimental values (1.0, 0.9 × KDP). This discrepancy is reasonable because the calculated value is based on a periodic and large crystal, while the experimental value depends on the quality and the size of the selected crystals.[68–70]

The SHG-weighted electron density (SHG density) of d_{31} was calculated to clarify the contributors of SHG intensity (Fig. 4a, b, d and e). For KBZFC, the empty electronic states of F 2p and Cl 3p are the dominant contributors to the SHG effect in the VB. In the CB, the unoccupied Zr 4d orbitals play a major role, together with the Ba 5d and F 2p orbitals to a small extent. For KBHFC, the empty electronic states of Cl 3p dominantly contribute to the SHG effect in the VB, and the empty electronic states of F 2p also contribute. In the CB, the unoccupied Ba 5d greatly contributes, the unoccupied Hf 5d offers few contributions, and F 2p orbitals provide very few contributions. Combining the SHG contribution densities of the VB and CB, the SHG-contributed percentages of the groups/ions are 60.71/33.12, 14.23/23.33, 25.48/43.81, and −0.43/−0.27% for MF_7, Ba^{2+}, Cl^-, and K^+ in KBZFC and KBHFC, respectively (Table S6†).

The results show that the MF_7 units and the Cl^- ions predominantly contribute to the SHG response. Ba^{2+} cations contribute much less to the lower ratio in the structure, and K^+ cations negatively contribute to SHG progress. Although Cl atoms connect to Ba atoms in KBZFC and KBHFC, the introduction of Cl^- ions increased the SHG intensity, which was demonstrated by the examples of KBZFC and KBHFC (1, 0.9 × KDP) *vs.* $K_3Ba_2Zr_6F_{31}$ (0.5 × KDP).

To develop this system, subsequent attempts can be made to obtain NCS halides with other F/Cl ratios or MF_xCl_y groups. KBZFC and KBHFC are positive uniaxial crystals with $n_e > n_o$ at 1064 nm. The calculation of linear optical properties indicates that KBZFC and KBHFC exhibit large birefringences (0.12, 0.10 @ 1064 nm) that are sufficient to satisfy the PM requirement and were proven by the shortest calculated PM wavelengths (Fig. S7e and f†), which may contribute to the 0D structure composed by isolated and ordered MF_7 units.

The theoretical birefringences at 546 nm are 0.12 for KBZFC and 0.10 for KBHFC, which are basically in alignment with the calculated birefringence values and are greatly enhanced compared with the reported DUV transparent fluorides $BaMgF_4$ (0.0077), $SrAlF_5$ (0.0242), $BaZnF_4$ (0.0164), Li_2CaMF_8 (M = Zr, Hf) (0.05, 0.03), and $K_3Ba_2Zr_6F_{31}$ (0.08).[41–45] The calculated electronic density difference (EDD) maps further illustrate the apparent charge transfer from Zr/Hf to F atoms and ordered dense electron cloud in the *ac* plane (Fig. 4c and f), which favors the superposition of optical anisotropy and illustrates the birefringence source of KBZFC and KBHFC.

Conclusions

$KBa_3M_2F_{14}Cl$ (M = Zr (KBZFC), Hf (KBHFC)), the NCS zirconium/hafnium halides, were synthesized with the incorporation of Cl atoms and firstly reported as NCS mixed metal halides that display DUV cutoff edge. KBZFC and KBHFC successfully achieve an optimal balance between several stringent criteria, that is, large SHG intensities (approximately 1.0, 0.9 × KDP), short UV cutoff edge extending to the DUV region, and sufficient birefringence (0.12, 0.10 @ 1064 nm). Apparently, KBZFC and KBHFC are promising NLO materials with a short UV cutoff edge, and they signify a new path for developing the next generation of NLO halides with a DUV cutoff edge.

Data availability

The experimental section, and additional tables and figures are available in the ESI.†

Author contributions

This work was conceptualised by M. Yan and R. L. Tang. Experimentation was performed by M. Yan. Software was executed by C. L. Hu and W. D. Yao. W. L. Liu contributed supervision. R. L. Tang and S. P. Guo contributed funding acquisition and supervision. The first draft of the manuscript

was prepared by M. Yan, and the final draft was edited by all the authors.

Conflicts of interest

The authors declare no competing financial interests.

Acknowledgements

The authors acknowledge the financial support from the National Natural Science Foundation of China (22071212 and 22101248), the Luyangjinfeng Talent Program of Yangzhou (YZLYJFJH2021YXBS083), and the Postgraduate Research & Practice Innovation Program of Jiangsu Province (KYCX22_3465).

Notes and references

1 X. Lu, Z. Chen, X. Shi, Q. Jing and M. H. Lee, *Angew. Chem., Int. Ed.*, 2020, **59**, 17648–17656.
2 Q. Q. Liu, X. Liu, L. M. Wu and L. Chen, *Angew. Chem., Int. Ed.*, 2022, **61**, e202205587.
3 X. H. Li, Z. H. Shi, M. Yang, W. L. Liu and S. P. Guo, *Angew. Chem., Int. Ed.*, 2022, **61**, e202115871.
4 X. H. Dong, L. Huang, H. M. Zeng, Z. Lin, G. H. Zou and K. M. Ok, *Angew. Chem., Int. Ed.*, 2022, **61**, e202116790.
5 G. H. Zou, H. Jo, S.-J. Lim, T.-S. You and K. M. Ok, *Angew. Chem., Int. Ed.*, 2018, **57**, 8619–8622.
6 W. F. Zhou and S. P. Guo, *Acc. Chem. Res.*, 2024, **57**, 648–660.
7 R. L. Tang, W. Xu, X. Lian, Y. Q. Wei, Y. L. Lv, W. L. Liu and S. P. Guo, *Small*, 2023, 2308348.
8 P. Yu, L. M. Wu, L. J. Zhou and L. Chen, *J. Am. Chem. Soc.*, 2014, **136**, 480–487.
9 Q. R. Ding, X. Y. Zhang, Z. S. Lin, Z. Y. Xiong, Y. S. Wang, X. F. Long, S. G. Zhao, M. C. Hong and J. H. Luo, *Sci. China: Chem.*, 2022, **65**, 1710–1714.
10 H. Y. Sha, J. X. Xu, Z. Y. Xiong, Z. J. Wang, R. B. Su, C. He, X. M. Yang, X. F. Long and Y. Liu, *Adv. Opt. Mater.*, 2022, **10**, 2200228.
11 X. Hao, M. Luo, C. S. Lin, G. Peng, F. Xu and N. Ye, *Angew. Chem., Int. Ed.*, 2021, **60**, 7621–7625.
12 X. F. Wang, Y. Wang, B. B. Zhang, F. F. Zhang, Z. H. Yang and S. L. Pan, *Angew. Chem., Int. Ed.*, 2017, **56**, 14119–14123.
13 Y. X. Ma, P. F. Li, C. L. Hu, J. G. Mao and F. Kong, *Adv. Sci.*, 2023, **10**, 2304463.
14 C. W. Xie, A. Tudi and A. R. Oganov, *Chem. Commun.*, 2022, **58**, 12491–12494.
15 H. T. Tian, N. Ye and M. Luo, *Angew. Chem., Int. Ed.*, 2022, **61**, e202200395.
16 C. Hu, M. Cheng, W. Q. Jin, J. Han, Z. H. Yang and S. L. Pan, *Research*, 2023, **6**, 0053.
17 T. T. Tran, H. W. Yu, J. M. Rondinelli, K. R. Poeppelmeier and P. S. Halasyamani, *Chem. Mater.*, 2016, **28**, 5238–5258.
18 W. Q. Huang, S. G. Zhao and J. H. Luo, *Chem. Mater.*, 2022, **34**, 5–28.
19 X. M. Liu, L. Kang, P. F. Gong and Z. S. Lin, *Angew. Chem., Int. Ed.*, 2021, **60**, 13574–13578.
20 T. T. Tran, J. Young, J. M. Rondinelli and P. S. Halasyamani, *J. Am. Chem. Soc.*, 2017, **139**, 1285–1295.
21 H. K. Liu, B. B. Zhang, L. Li and Y. Wang, *ACS Appl. Mater. Interfaces*, 2021, **13**, 30853–30860.
22 L. Kang, P. F. Gong, Z. S. Lin and B. Huang, *Angew. Chem., Int. Ed.*, 2021, **60**, 16680–16686.
23 C. T. Chen, G. L. Wang, X. Y. Wang and Z. Y. Xu, *Appl. Phys. B*, 2009, **97**, 9–25.
24 Y. Q. Li, F. Liang, S. G. Zhao, L. Li, Z. Y. Wu, Q. R. Ding, S. Liu, Z. S. Lin, M. C. Hong and J. H. Luo, *J. Am. Chem. Soc.*, 2019, **141**, 3833–3837.
25 B. Q. Yuan, H. P. Wu, Z. G. Hu, J. Y. Wang, Y. C. Wu and H. W. Yu, *Chem. Mater.*, 2022, **34**, 8004–8012.
26 S. Bai, X. D. Zhang, B. B. Zhang, L. Li and Y. Wang, *Inorg. Chem.*, 2021, **60**, 10006–10011.
27 P. F. Gong, L. Kang and Z. S. Lin, *J. Am. Chem. Soc.*, 2020, **142**, 15157–15163.
28 Q. Wang, W. Song, Y. Lan, L. L. Cao, L. Huang, D. J. Gao, J. Bi and G. H. Zou, *Inorg. Chem. Front.*, 2022, **9**, 3590–3597.
29 W. Z. Zhao, Y. N. Zhang, Y. Z. Lan, J. W. Cheng and G. Y. Yang, *Inorg. Chem.*, 2022, **61**, 4246–4250.
30 M. F. Wu, J. W. Feng, C. W. Xie, A. Tudi, D. D. Chu, J. J. Lu, S. L. Pan and Z. H. Yang, *ACS Appl. Mater. Interfaces*, 2022, **14**, 39081–39090.
31 L. Xiong, J. Chen, J. Lu, C. Y. Pan and L. M. Wu, *Chem. Mater.*, 2018, **30**, 7823–7830.
32 Y. L. Zhou, X. Y. Zhang, Z. Y. Xiong, X. F. Long, Y. Q. Li, Y. X. Chen, X. Chen, S. G. Zhao, Z. S. Lin and J. H. Luo, *J. Phys. Chem. Lett.*, 2021, **12**, 8280–8284.
33 H. N. Liu, H. P. Wu, Z. G. Hu, J. Y. Wang, Y. C. Wu, P. S. Halasyamani and H. W. Yu, *ACS Mater. Lett.*, 2023, **5**, 155–161.
34 T. T. Tran, N. Z. Koocher, J. M. Rondinelli and P. S. Halasyamani, *Angew. Chem., Int. Ed.*, 2017, **56**, 2969–2973.
35 H. P. Wu, B. B. Zhang, H. W. Yu, Z. G. Hu, J. Y. Wang, Y. C. Wu and P. S. Halasyamani, *Angew. Chem., Int. Ed.*, 2020, **59**, 8922–8926.
36 M. Xia, F. M. Li, M. Mutailipu, S. J. Han, Z. H. Yang and S. L. Pan, *Angew. Chem., Int. Ed.*, 2021, **60**, 14650–14656.
37 M. Mutailipu, J. Han, Z. Li, F. M. Li, J. J. Li, F. F. Zhang, X. F. Long, Z. H. Yang and S. L. Pan, *Nat. Photonics*, 2023, **17**, 649–701.
38 H. T. Qiu, F. M. Li, C. C. Jin, Z. H. Yang, J. J. Li, S. L. Pan and M. Mutailipu, *Angew. Chem., Int. Ed.*, 2023, **63**, e202316194.
39 H. T. Qiu, S. L. Pan and M. Mutailipu, *Fundam. Res.*, 2023, DOI: **10.1016/j.fmre.2023.08.017**.
40 M. Mutailipu, K. R. Poeppelmeier and S. L. Pan, *Chem. Rev.*, 2021, **121**, 1130–1202.
41 Y. Z. Tong, X. Y. Meng, Z. Z. Wang, C. T. Chen and M. H. Lee, *J. Appl. Phys.*, 2005, **98**, 033504.
42 H. Huang, Z. S. Lin, L. Bai, R. He and C. T. Chen, *Solid State Commun.*, 2010, **150**, 2318–2321.
43 G. Jian, M. Liu, W. Chen, C. Yan and C. P. Wong, *Opt. Mater.*, 2018, **86**, 471–474.
44 M. Yan, R. L. Tang, W. Xu, W. L. Liu and S. P. Guo, *Inorg. Chem.*, 2024, **63**, 5260–5268.

45 M. Yan, R. L. Tang, W. D. Yao, W. L. Liu and S. P. Guo, *Chem. Sci.*, 2024, **15**, 2883–2888.
46 X. L. Cao, C. L. Hu, F. Kong and J. G. Mao, *Inorg. Chem.*, 2015, **54**, 3875–3882.
47 H. Jo, M. H. Lee and K. M. Ok, *Chem. Mater.*, 2021, **33**, 1875–1882.
48 M. J. Xia, X. X. Jiang, Z. S. Lin and R. K. Li, *J. Am. Chem. Soc.*, 2016, **138**, 14190–14193.
49 K. A. Gayvoronskaya, N. A. Didenko, A. B. Slobodyuk, A. V. Gerasimenko and V. Y. Kavun, *J. Fluorine Chem.*, 2011, **132**, 1159–1164.
50 R. B. Fu, X. Y. Zhang, Z. Zhou, W. X. Bao, H. X. Tang, Z. J. Ma and X. T. Wu, *Chem. Sci.*, 2023, **14**, 136–142.
51 Y. Huang, X. G. Meng, P. F. Gong, Z. S. Lin, X. G. Chen and J. G. Qin, *J. Mater. Chem. C*, 2015, **3**, 9588–9593.
52 X. L. Chen, Q. Jing and K. M. Ok, *Angew. Chem., Int. Ed.*, 2020, **59**, 20712.
53 Q. Wu, X. G. Meng, C. Zhong, X. G. Chen and J. G. Qin, *J. Am. Chem. Soc.*, 2014, **136**, 5683–5686.
54 G. Zhang, Y. J. Li, K. Jiang, H. Y. Zeng, T. Liu, X. G. Chen, J. G. Qin, Z. S. Lin, P. Z. Fu, Y. C. Wu and C. T. Chen, *J. Am. Chem. Soc.*, 2012, **134**, 14818–14822.
55 Q. Wu, X. Liu, F. Liang, S. R. Xu, H. B. Pi, X. Han, Y. Liu, Z. S. Lin and Y. J. Li, *Dalton Trans.*, 2019, **48**, 13529–13535.
56 J. J. Zhou, Y. Q. Liu, H. P. Wu, H. W. Yu, Z. S. Lin, Z. G. Hu, J. Y. Wang and Y. C. Wu, *Angew. Chem., Int. Ed.*, 2020, **59**, 19006–19010.
57 I. D. Brown and D. Altermatt, *Acta Crystallogr., Sect. B: Struct. Sci.*, 1985, **41**, 244–247.
58 J. G. Ballard, T. Birchall and D. R. Slim, *J. Chem. Soc., Dalton Trans.*, 1977, 1469–1472.
59 U. Müller, *Z. Anorg. Allg. Chem.*, 1979, **454**, 75–81.
60 H. Preiss, *Z. Anorg. Allg. Chem.*, 1966, **346**, 272–278.
61 M. Rolf, K. Detlef and P. Hans, *Z. Naturforsch., B: J. Chem. Sci.*, 1994, **49**, 1–4.
62 R. Minkwitz, A. Kornath and H. Preut, *Z. Anorg. Allg. Chem.*, 1994, **620**, 638–641.
63 P. F. Gong, Y. Yang, F. G. You, X. Y. Zhang, G. M. Song, S. Z. Zhang, Q. Huang and Z. S. Lin, *Cryst. Growth Des.*, 2019, **19**, 1874–1879.
64 G. Wang, H. M. Liu, X. X. Jiang, L. Yang, Z. S. Lin, Z. G. Hu, X. G. Meng, X. G. Chen and J. G. Qin, *Chin. J. Inorg. Chem.*, 2017, **33**, 2117–2123.
65 T. K. Jiang, S. N. Yan, C. L. Hu, Y. F. Li, F. Kong and J. G. Mao, *Inorg. Chem.*, 2022, **61**, 4801–4805.
66 S. K. Kurtz and T. T. Perry, *J. Appl. Phys.*, 1968, **39**, 3798–3813.
67 H. Y. Sha, Y. R. Shang, Z. J. Wang, R. B. Su, C. He, X. M. Yang and X. F. Long, *Small*, 2023, e2309776, DOI: **10.1002/smll.202309776**.
68 Y. X. Ma, Y. P. Gong, C. L. Hu, F. Kong and J. G. Mao, *Inorg. Chem.*, 2020, **59**, 7852–7859.
69 R. L. Tang, M. Yan, W. D. Yao, W. L. Liu and S. P. Guo, *Inorg. Chem.*, 2022, **61**, 2333–2339.
70 M. L. Liang, Y. X. Ma, C. L. Hu, F. Kong and J. G. Mao, *Chem. Mater.*, 2020, **32**, 9688–9695.